Interplanetary coronal mass ejection and ambient interplanetary magnetic field correlations during the Sun-Earth connection events of October–November 2003

C. J. Farrugia,[1] H. Matsui,[1] H. Kucharek,[1] R. B. Torbert,[1] C. W. Smith,[1] V. K. Jordanova,[1] K. W. Ogilvie,[2] R. P. Lepping,[2] D. B. Berdichevsky,[2] T. Terasawa,[3] J. Kasper,[4] T. Mukai,[5] Y. Saito,[5] and R. Skoug[6]

Received 7 December 2004; revised 9 July 2005; accepted 14 July 2005; published 30 September 2005.

[1] Magnetic field observations made during 28 October to 1 November 2003, which included two fast interplanetary coronal mass ejections (ICMEs), allow a study of correlation lengths of magnetic field parameters for two types of interplanetary (IP) structures: ICMEs and ambient solar wind. Further, they permit the extension of such investigations to the magnetosheath and to a distance along the Sun-Earth line (X) of about 400 R_E. Data acquired by three spacecraft are examined: ACE, in orbit around the L1 point; Geotail, traveling eastward in the near-Earth solar wind (at R $\sim$ 30 R_E); and Wind, nominally in the distant geomagnetic tail (R ~ -160 R_E) but making repeated excursions into the magnetosheath/solar wind due to the flapping of the tail. Analyses are presented in both time and frequency domains. We find significant differences in the cross-correlation/coherence properties of the ambient interplanetary magnetic field (IMF) and ICME parameters. For the ambient IMF, we find high coherence to be confined to low frequencies, consistent with other studies. In contrast, ICME magnetic field parameters remain generally coherent up to much higher frequencies. Scale lengths of ICME magnetic field parameters are in excess of 400 R_E. High speeds of $\sim$1700 km s^{-1} are inferred from the plot of phase difference versus frequency, consistent with that obtained from plasma instruments. To strengthen these results and to extend them to include dependence on the distance perpendicular to the Sun-Earth line (Y), we examine a 28-day interval in year 2001 characterized by a sequence of 10 ICMEs and containing roughly equal ambient solar wind and ICME time intervals. ACE-Wind X and Y separations were $\sim$220 and $\sim$250 R_E, respectively. We find good coherence/correlation alternating with poor values. In particular, we find that in general ICME coherence/correlation lengths along Y are larger by a factor of 3–5 than those quoted in the literature for ambient solar wind parameters. Our findings are good news for the space weather effort, which depends crucially on predicting the arrival of large events, since they make possible the placement of upstream monitors to give a longer lead time than at L1.

Citation: Farrugia, C. J., et al. (2005), Interplanetary coronal mass ejection and ambient interplanetary magnetic field correlations during the Sun-Earth connection events of October–November 2003, *J. Geophys. Res.*, *110*, A09S13, doi:10.1029/2004JA010968.

1. Introduction

[2] A major aim motivating investigations of cross-correlations and length scales of parameters of the interplanetary magnetic field (IMF) and solar wind is to determine how far along the Sun-Earth line, and perpendicular to it, can we place an upstream monitor and still be able to predict reliably the interplanetary conditions that affect the magnetosphere. Clearly, the larger the distance, the longer the lead time. However, this can be counterbalanced by increasing inaccuracy.

[3] Much of the success of the space weather program depends on predicting the arrival and properties (for exam-

[1]Institute for the Study of Earth, Oceans and Space, University of New Hampshire, Durham, New Hampshire, USA.
[2]NASA Goddard Space Flight Center, Greenbelt, Maryland, USA.
[3]Department of Earth and Planetary Science, University of Tokyo, Tokyo, Japan.
[4]Center for Space Research, Massachusetts Institute of Technology, Cambridge, Massachusetts, USA.
[5]Japan Aerospace Exploration Agency, Kanagawa, Japan.
[6]Los Alamos National Laboratory, Los Alamos, New Mexico, USA.

0148-0227/05/2004JA010968$09.00

ple, duration and average strength of a southward component of the magnetic field) of large events such as interplanetary coronal mass ejections (ICMEs, also called "ejecta" hereunder) and their subclass, magnetic clouds. (The latter are configurations in which a magnetic field of above-average strength rotates smoothly through a large angle in a plasma of low beta [*Burlaga et al.*, 1981]). Several studies have shown that these events are responsible for the largest disturbances in the terrestrial magnetosphere-ionosphere system (*Zhang and Burlaga* [1987], *Tsurutani et al.* [1988], *Gosling et al.* [1990, 1991], *Richardson et al.* [2002], and *Farrugia et al.* [2005]; see also review by *Farrugia et al.* [1997] and references therein). While typical correlation studies have addressed ambient IMF and solar wind parameters separately [*Russell et al.*, 1980; *Crooker et al.*, 1982; *Kelly et al.*, 1986; *Paularena et al.*, 1998; *Richardson et al.*, 1998; *Collier et al.*, 1998; *Coplan et al.*, 2001], they are sometimes considered in combination [*Richardson and Paularena*, 2001; *Matsui et al.*, 2002]. No attempt has been undertaken to distinguish the results by interplanetary (IP) structure.

[4] The violent Sun-Earth connection events of October–November 2003, forming the focus of this Special Issue, are particularly suited to extend our knowledge of correlation lengths of large structures. This is because two ICMEs occurred in quick succession during 29 October to 1 November 2003. Further, there were three spacecraft spread out widely in the Sun-Earth (X) direction: ACE was orbiting around the L1 libration point ($\sim$235 Earth radii, R_E), Geotail was at least for some of the time (encompassing the entire passage of the first ICME) traversing the near-Earth solar wind, and Wind was at ~ -160 R_E, nominally near midtail but making repeated excursions into the magnetosheath/solar wind because of the special conditions prevailing during this time period. The ACE-Wind separation was thus of order 400 R_E, and this affords a good opportunity to study correlation lengths over almost twice the L1 distance, once the intervals inside the magnetosheath can be determined and the effect of the bow shock taken into account. This fulfills one of the aims of Wind's excursion to the L2 point from October 2003 to February 2004.

[5] We propose a study of correlation coefficients and length scales for 28 October to 1 November 2003. We shall investigate the correlations of parameters of ICMEs and the ambient solar wind quantities separately, concentrating on the magnetic field parameters. We shall also analyze the data in both time and frequency domains. An early application of the latter technique (spectral analysis) in a space physics context was made by *Holmgren and Kintner* [1990], who studied ionospheric inhomogeneities with an interferometric technique using data from two Langmuir probes. *Matsui et al.* [2002] applied it to a large-scale study on the coherence of interplanetary parameters observed by Wind and ACE over 1 year (1999). Time series and spectral analyses are complementary to each other, but spectral analysis has the added advantage of identifying the frequency range of the fluctuations that remain coherent when propagating from one spacecraft to the other.

[6] We obtain generally contrasting results for ICME and ambient IMF correlation/coherence length scales for 28 October to 1 November 2003. We then examine the matter further by examining ACE-Wind observations in another interval, this time in 2001. The chosen period (26 March to 23 April 2001) represents a very active interval both on the Sun, which is related to a large sunspot group consisting of three or more active regions [see *Berdichevsky et al.*, 2003], as well as at 1 AU, where a sequence of 10 transients, responsible for several intense geomagnetic storms, passed Earth within $\sim$1 month. We find a correlation coefficient which episodically reaches large values ($\sim$0.9), peaking in rough synchrony with ejecta intervals documented in other studies [*Cane and Richardson*, 2003; *Zhang et al.*, 2004]. In this example, spacecraft Wind was to the west of Earth (Y [GSE] < 0) while executing a distant prograde orbit. The ACE-Wind separation vector was (219 ± 3.4, 247.7 ± 19.1, -17.9 ± 1.7) R_E, making for a total separation of $\sim$330 R_E. Spectral analysis shows that generally, the coherence of ejecta parameters persists up to higher frequencies, in sharp contrast to that of ambient solar wind parameters. There are, however, some exceptions to this, where the coherence is very low even for ejecta.

[7] A major conclusion is that contrary to ambient IMF and solar wind parameters, where the correlation length is of order 40–70 R_E in the Y direction [*Crooker et al.*, 1982; *Richardson and Paularena*, 2001] we obtain generally much higher correlations over linear dimension in Y of at least $\sim$248 R_E in the case of the ICMEs.

[8] The layout of the paper is as follows. We summarize the two techniques in section 2. Sections 3 and 4 are devoted to analyses of the Halloween 2003 events in the time and frequency domains, respectively. Section 5 examines the control interval in 2001. We then draw conclusions and discuss the results in section 6.

2. Technique

[9] We analyze correlations and lag times of signals at different sites by two satellites in both time and frequency domains using cross-correlation and spectral analyses [see *Press et al.*, 1992, and references therein; *Eriksson*, 1998]. To analyze in the time domain, we follow the approach discussed in detail by *Richardson et al.* [1998]. Briefly, we have two time series of some IP parameter (say, B_z), one series at the upstream monitor (ACE) and another at the downstream monitor (Geotail or Wind). The data series are first despiked. The data resolutions of the two time series are then equalized by linear interpolation. Data blocks of 12 hours' duration, overlapped by one half, are taken at a time. The one from measurements at the upstream monitor is shifted forward in time by the convection (advection) delay to map it to the corresponding time at the downstream monitor. The convection delay is given by $\Delta X/V_x$, where ΔX is the X-separation of the probes and V_x is the average solar wind velocity along X in these 12 hours. The two series are then cross-correlated as a function of lag. Length scales may be obtained from this procedure, even though their definition is somewhat arbitrary. We can define a length scale as corresponding to the distance over which the cross-correlation coefficient R degrades "significantly." *Richardson and Paularena* [2001] suggest a decrease by 0.1, and we shall adhere to this choice here.

[10] Spectral analysis is based on three quantities, the amplitude ratio, the coherence between the signals, and their

phase difference. We follow the treatment of *Holmgren and Kintner* [1990] (see also *Bendat and Piersol* [1971] and *Eriksson* [1998] as elaborated in an IP context by *Matsui et al.* [2002]). Let $Q_{Wind}(f)$ and $Q_{ACE}(f)$ represent the Fourier components of a specific IP parameter we wish to study. The amplitude ratio, $R(f)$ is defined by

$$R(f) = \sqrt{\frac{\sum_{i=1}^{N} |Q_{i,ACE}(f)|^2}{\sum_{i=1}^{N} |Q_{i,Wind}(f)|^2}}, \quad (1)$$

where N is the number of fast fourier transforms (FFTs) used to compute this quantity (in general, 4, see below). The coherence C(f) is a real number ($0 \leq C(f) \leq 1$) defined by

$$C(f) = \frac{\left|\sum_{i=1}^{N} \left(Q_{i,ACE}(f) Q^{\star}_{i,Wind}(f)\right)\right|^2}{\left(\sum_{i=1}^{N} |Q_{i,ACE}(f)|^2\right)\left(\sum_{i=1}^{N} |Q_{i,Wind}(f)|^2\right)}, \quad (2)$$

The star symbol stands for complex conjugation. (In this paper we use the term "coherence" as the quantity one obtains from equation (2).) The coherence concept makes sense only when the signals are stationary. Finally, the phase difference $\Delta\Phi(f)$ between the Fourier components $Q_{i,ACE}(f)$ and $Q_{i,Wind}(f)$ is given by

$$\Delta\Phi(f) = arg\left(\sum_{i=1}^{N} \left[Q_{i,ACE}(f) Q^{\star}_{i,Wind}(f)\right]\right), \quad (3)$$

where "arg" is the argument of the complex function within the square brackets.

[11] The coherence is determined by the constancy of the phase of the numerator in equation (2). Randomly distributed phases implies C = 0. A low coherence at some frequency implies that at that frequency the two signals are not correlated at the two measuring points and/or not stationary in time.

[12] The phase difference $\Delta\Phi(f)$ contains information about the propagation of the IMF and solar wind parameters between the two monitors. Of interest are those cases where the coherence is high. Suppose we have a wave field varying as $\exp(2\pi i[x/\lambda - ft])$. The phase difference at two observing point a distance ΔX apart is

$$\Delta\Phi = \frac{2\pi\Delta X}{\lambda} = \frac{2\pi\Delta X}{v_\phi} f, \quad (4)$$

where $v_\phi = f\lambda$ denotes the phase speed. Thus λ or v_ϕ may be computed from the phase spectrum. This is particularly useful in the present application since the extraordinarily high velocities measured during October–November 2003 events were subject to some uncertainty (see below and *Skoug et al.* [2004]), and it would be desirable to obtain some independent confirmation of them. This technique is able to do this.

[13] The numerical procedure used to produce the frequency-time spectra is the same as that explained by *Matsui et al.* [2002], to which we refer the reader for further details. Briefly, an FFT is carried out on the signal of a physical quantity (say, B_z) at each spacecraft. The quantities $R(f)$, $C(f)$, and $\Delta\Phi(f)$, defined above, are then calculated. We use 1 min averaged data in the calculation of cross-spectra. The number n of data points per FFT is set equal to 512, i.e., 512 min per FFT. The number N of FFTs is chosen to be 4, to strike a balance between random errors, which increase with fewer FFTs [*Benignus*, 1969], and time resolution, which decreases with more FFTs. Neighboring FFTs are overlapped by one-half so that each cross-spectrum is based on 1280 data points (21.3 hours).

3. Observations

3.1. ACE

[14] For the 5-day period 28 October to 1 November, Figure 1 shows ACE/SWEPAM plasma [*McComas et al.*, 1998] and ACE/MAG magnetic field [*Smith et al.*, 1998] observations. ACE was situated at (231, 41, −21) R_E and (232, 41, −20) R_E (GSE coordinates) at the start and end of the period shown, respectively. From top to bottom, the panels display the proton density, bulk speed, temperature, and dynamic pressure, the total field, and its GSM components, the plasma beta (ratio of plasma to magnetic pressure), the ϵ parameter, and the clock angle θ of the IMF (i.e., the polar angle in the GSM (YZ) plane). The data resolution is 16 s for the magnetic field and 64 s for the plasma data. The energy-coupling function ϵ represents the fraction of the Poynting flux entering the magnetosphere [*Perreault and Akasofu*, 1978] and is expressed here in mW m^{-2}. From general considerations of reconnection, *Kan and Lee* [1979], following *Sonnerup* [1974], showed that ϵ is proportional to the power input per m^2 to the magnetosphere from the solar wind.

[15] There are (1) data gaps in n_p (and P_D), and (2) the plasma data coverage is at lower resolution from ~1300 UT, 28 October to ~2200 UT, 30 October. The SWEPAM operations were affected by (1) penetrating radiation from an intense solar energetic particle event associated with the first ICME, and (2) for several of the highest-speed data points on 29–30 October, the high-energy part of the solar wind beam exceeded the energy range when operating in search mode. These points are discussed in detail by *Skoug et al.* [2004], to which we refer the reader.

[16] At least two shocks are present in the interval considered, passing ACE at ~0600 UT (29 October) and 1600 UT (30 October) (marked S_1, S_2). (Henceforth we use the notation x UT (y) to designate x UT on y October 2003.) Each is followed within a few hours by a long interval characterized by strong magnetic fields and large rotations of the magnetic field vector. In the case of S_2, high values of He^{++}/H^{+} (~30%) were recorded between 0000 UT (31) and 1200 UT (2) (not shown) [see *Skoug et al.*, 2004, Figure 3]. These and other signatures [see *Skoug et al.*, 2004; *Malandraki et al.*, 2005] indicate the presence of two ICMEs. Basing ourselves principally on the magnetic field data shown in Figure 1, we take the ICME 1 interval to stretch from 1000 UT (29) up to 0200 UT (30). The arrival time of the leading edge agrees with *Malandraki et al.*

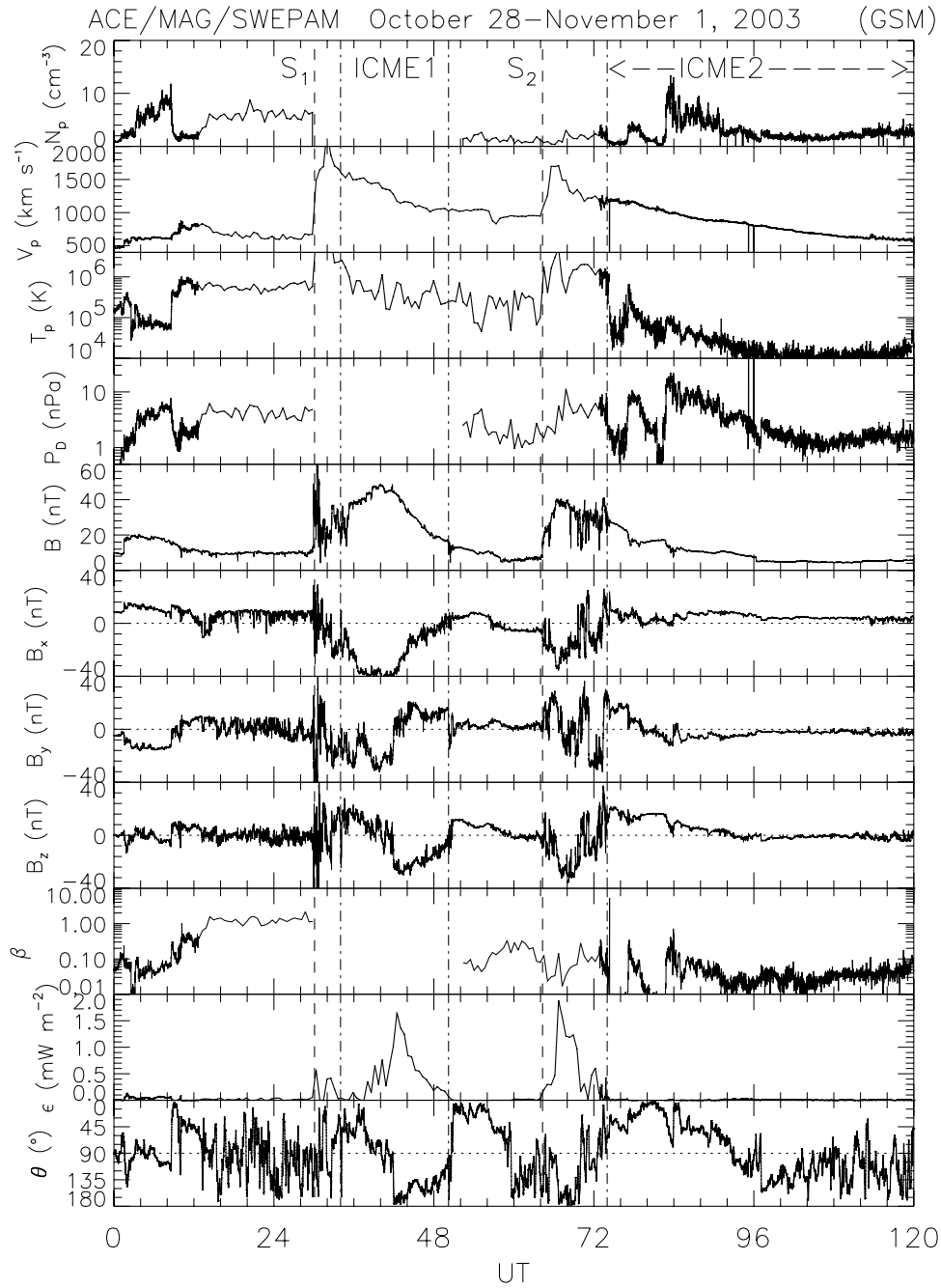

Figure 1. ACE plasma and and magnetic field observations for the 5-day interval 28 October to 1 November 2003. The temporal resolution of the data is 16 s (field) and (nominally) 64 s (plasma). From top to bottom, the panels show the proton density, bulk speed, temperature, and dynamic pressure, the total field and its components in GSM coordinates, the proton beta, the "ϵ" parameter, and the IMF clock angle.

[2005], but the rear end is some hours earlier and coincides in our case with a clear magnetic field discontinuity. ICME 2 starts at 0200 UT (31) and goes on all the way to 2400 UT (1). The starting point agrees with that of *Skoug et al.* [2004] and *Malandraki et al.* [2005]. There is uncertainty in the literature on the timing of its rear edge [*Malandraki et al.*, 2005], and possibly it can be as late as 1800 UT (2). Thus we shall discuss ICME 2 only qualitatively.

[17] A distinguishing feature of these events is the unusually high velocities reached, to well above 1500 km s^{-1}. These extraordinary values lead to a rapid transit to 1 AU comparable to the rapidity with which solar disturbances reached Earth following the historic flare observed by Carrington in September 1859 [*Carrington*, 1859; see also *Tsurutani et al.*, 2003]. Worth noting are the two large discrete bursts in the power deposition into the magneto-

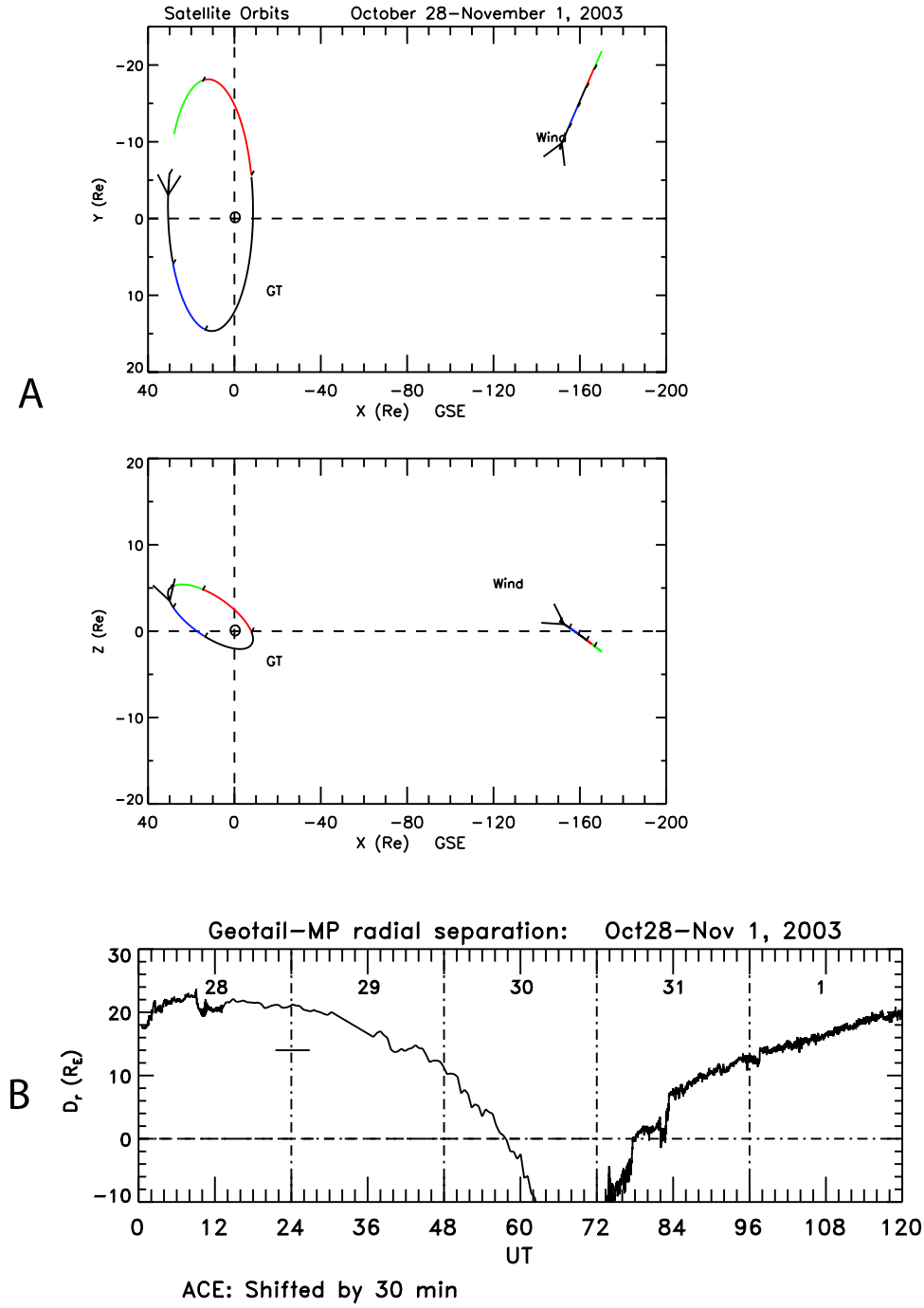

Figure 2. (a) Orbits of the near-Earth spacecraft Geotail (GT) and Wind for 28 October to 1 November 2003. Different days are marked by different colors. (top) Projection onto the GSE (XY) plane; (bottom) projection onto the GSE (XZ) plane. (b) The radial distance (D_r) of Geotail from the model magnetopause of *Shue et al.* [1998], where the interplanetary B_z and P_D have been shifted forward in time by the average propagation delay from ACE to Geotail. Positive D_r indicates that GT is outside the magnetopause.

sphere (penultimate panel) and the virtual absence of activity in the ~1/2 day separating the ICMEs. With the ICME durations given, it appears that the two bursts of large powering of the magnetosphere had different causes: the first was due to the $B_Z < 0$ phase of the first ejecta, and the second was due to the sheath region ahead of the second ejecta.

3.2. Geotail

[18] For this 5-day period, Figure 2a shows the orbits of the near-Earth spacecraft Geotail and Wind in GSE XY (top) and XZ projections. In the figure, the Sun is to the left. The different days are marked by different colors. To determine when Geotail is outside the magnetosphere, Figure 2b shows the radial distance of the spacecraft from

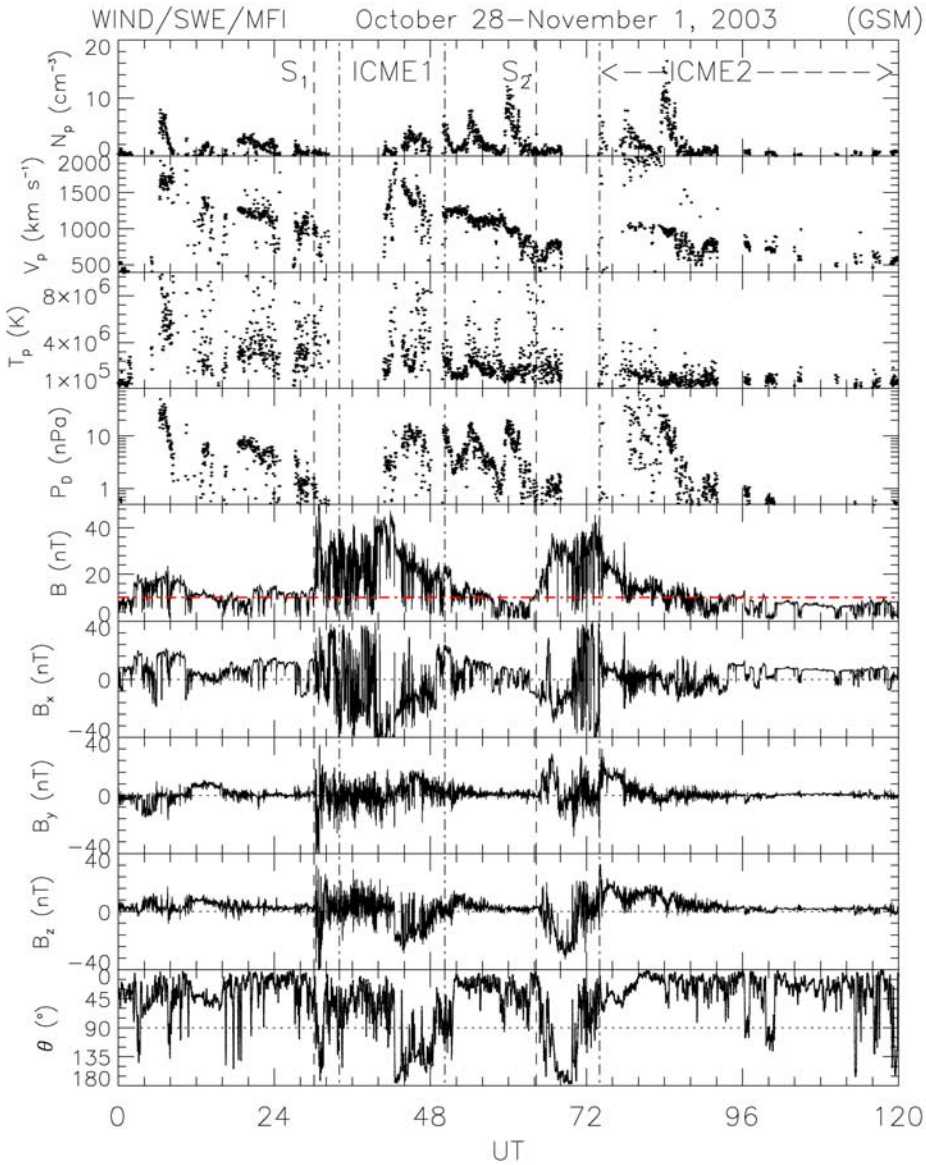

Figure 3. Plasma and magnetic field measurements from Wind for 28 October to 1 November 2003. The data resolutions are 3 s for the magnetic field and 97 s for the plasma parameters. Plotted are the proton number density, bulk speed, temperature and dynamic pressure, the total field, the GSM components of the magnetic field, and the IMF clock angle. Wind is located at X ≈ -160 R_e on the duskside.

the model magnetopause of *Shue et al.* [1998], which takes into account both the north-south component of the IMF, B_z, as well as the dynamic pressure, P_D. The spacecraft is in the solar wind/magnetosheath from 0000 UT (28) to ~1000 UT (30), and again from ~1000 UT (31) onward.

3.3. Wind

[19] Spacecraft Wind was crossing the ecliptic plane at a downtail distance which increased from -150 R_E to -170 R_E (Figure 2a). Its main motion was across the dawnward side of the geomagnetic tail with Y decreasing from -9 R_E to -22 R_E. The geomagnetic latitude (MLAT) varied between 4° and 25°.

[20] Figure 3 shows the Wind measurements from the SWE [*Ogilvie et al.*, 1995] and the MFI [*Lepping et al.*, 1995] Investigations for 28 October to 1 November 2003. Plotted from top to bottom are the proton number density, bulk speed, temperature and dynamic pressure, the total field and its GSM components, and the clock angle. The data resolution is 3 s for the magnetic field and nominally 97 s for the plasma parameters. (The dot-dash horizontal line drawn at $B = 10$ nT in the B-panel is explained below.) For reference, the times of arrival of the shocks S1 and S2 and the durations of the ICMEs at ACE are shown in the top panel. The plasma data coverage is sparse for long intervals. The reason for this is that during the October–November

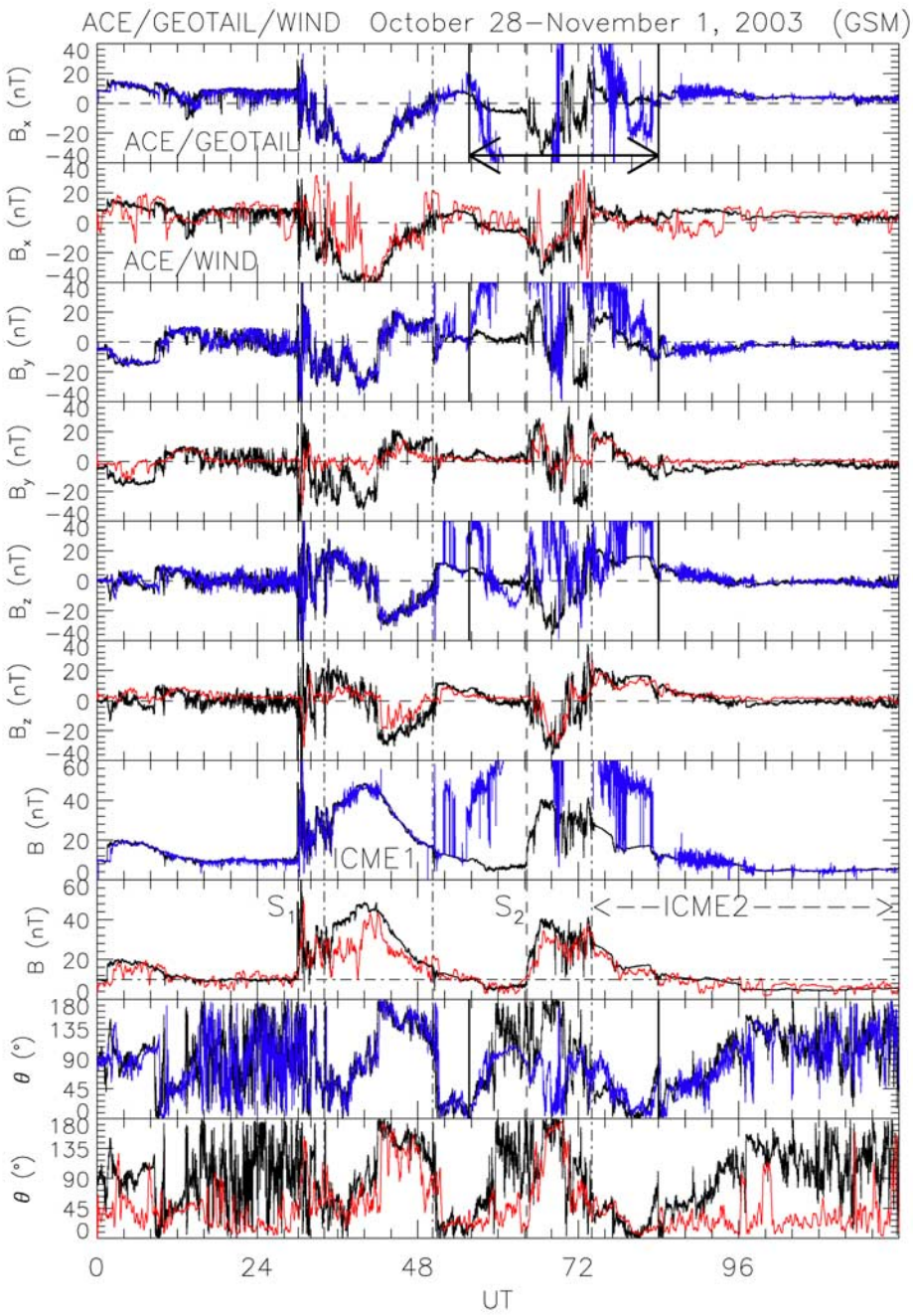

Figure 4. Pairwise overlays of ACE/Geotail (black/blue) and ACE/Wind (black/red) magnetic field parameters. ACE data are shown by black traces in all the panels. From top to bottom: B_x, B_y, B_z, B, and the clock angle. The Wind data are 15 min smoothed averages of the actual measurements. Geotail data are 12.4 s averages.

period, Wind was generally in the tail, heading downstream to the L2 point. While Wind is in the tail, the plasma flow is so slow that the Faraday Cups in the SWE instrument (which are designed for flows >200 km s^{-1}) do not generally see the plasma; sometimes the flow will drift into its field of view but mainly not.

[21] Nominally, at these distances, Wind would be in the dawnside plasma sheet, but the extreme conditions on this day made the tail "flap" erratically, as inferred, for example, from the large-amplitude **B**-fluctuations during the passages of the two ICMEs, making the spacecraft reside alternately in the tail and magnetosheath/solar wind. Even so, one may note that visually, there is a strong similarity between the trends (envelopes) in the profiles of magnetic field parameters at Wind and ACE (Figure 1), and comparable extreme values of the magnetic field are measured on

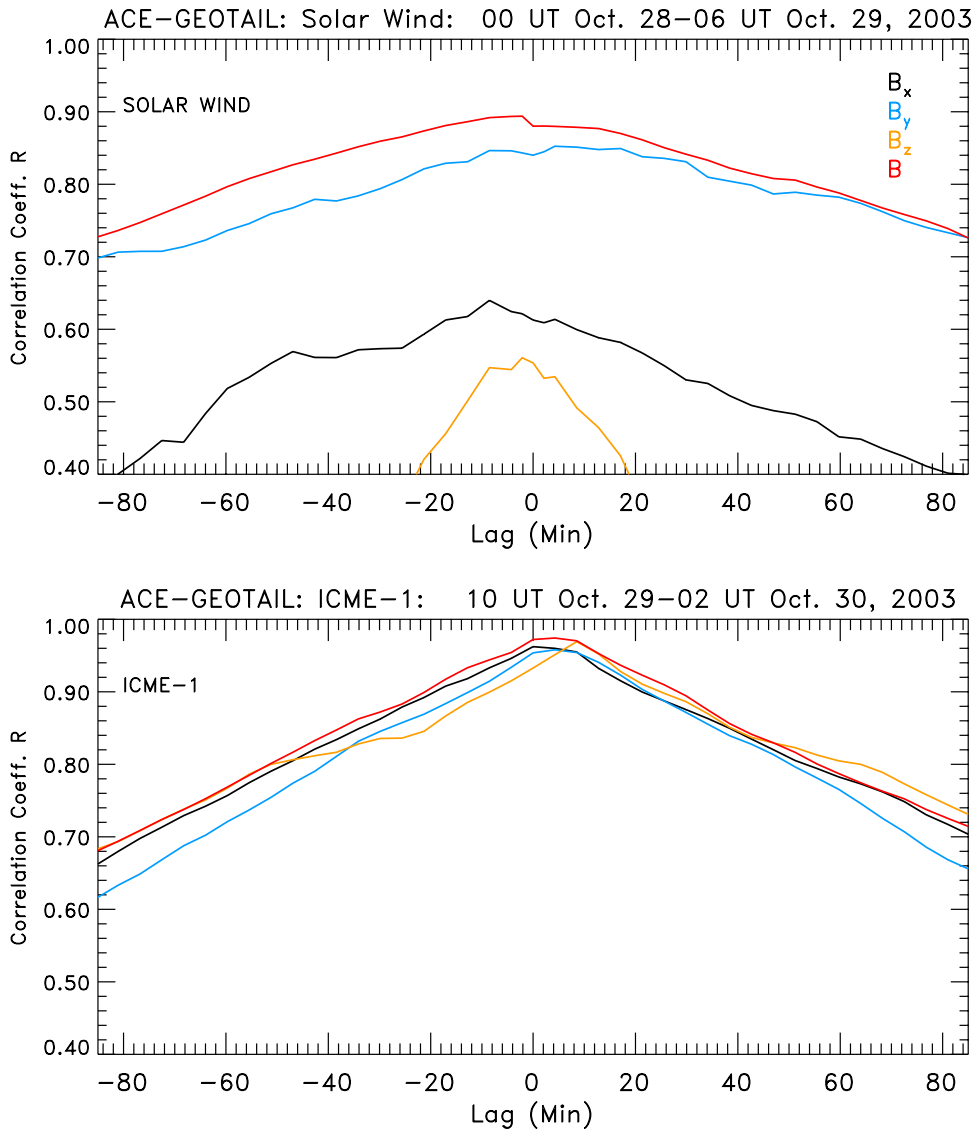

Figure 5. Values of the ACE-Geotial cross-correlation coefficients for magnetic field parameters in the time intervals indicated at the top of each panel. (top) Solar wind; (bottom) ICME 1. For further details, see text.

both spacecraft. The high speeds behind the first ICME observed at ACE are also recorded at Wind when the spacecraft is in the outer magnetosheath or solar wind. Note the large-amplitude variations in the dynamic pressure, P_D, on 30 October, during the period between the two ICMEs.

[22] We shall need to use those data acquired by the spacecraft when it resides in the magnetosheath or in the solar wind. We shall proceed as follows. We take 15 min averages of the data to smooth over passages through the tail and thus obtain the magnetosheath/solar wind values approximately. (The quality of the resulting correlation may be seen in the time series of Figure 4 below.) We then remove any residual tail values using theory combined with earlier ISEE 3 observations as follows. At Wind's distance of $\sim -160\ R_E$, the geomagnetic tail has typically reached its asymptotic radius and the magnetic field strength approached the value of 10 nT [*Coroniti and Kennel*, 1972; *Slavin et al.*, 1985]. This value is indicated by the horizontal line in the *B*-panel. In particular, one may note a continued residence in the tail approximately coinciding with the time interval between the end of ICME 1 and S_2 ($\sim$0400–1600 UT (30)) and during most of the Earth passage of ICME 2. All values less than 10 nT are removed in the correlations that follow, as an approximate way of weeding out the measurements made in the tail. No cross-correlations ACE-Wind for ICME 2 are attempted.

4. Time Series and Spectral Analyses

4.1. Time Series Analysis

[23] Figure 4 overlays ACE/Geotail (black-blue traces) and ACE/Wind (black-red traces) profiles of magnetic field parameters. Geotail field data are from the MGF instrument [*Kokubun et al.*, 1994] plotted at a time resolution of 12.4 s. The Wind measurements are shown averaged over 15 min, as discussed above. For reference, we have marked in the *B*-

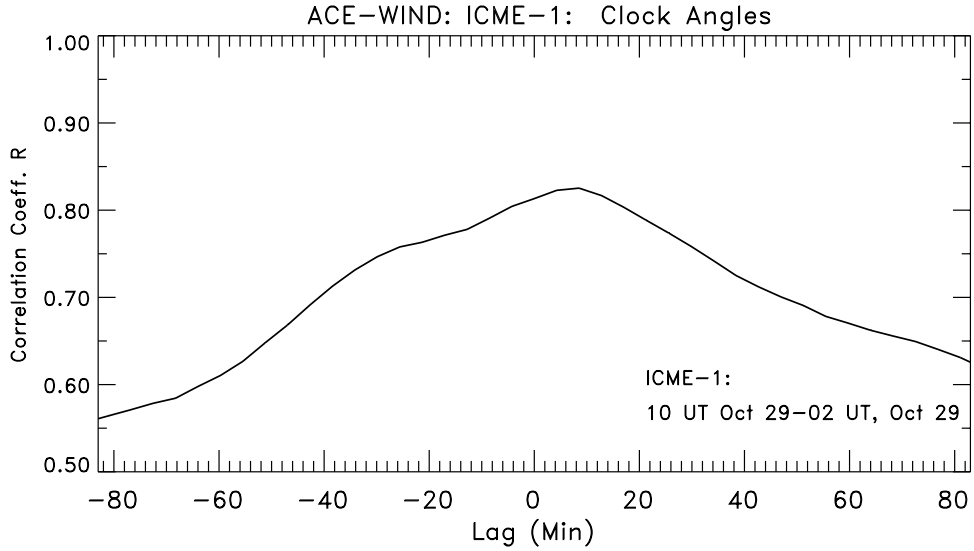

Figure 6. Cross-correlation coefficient of the clock angles from ACE and Wind as a function of lag for ICME 1.

panels the times of the two shocks and the durations of the ICMEs as observed at ACE.

4.1.1. ACE-Geotail

[24] Consider now the ACE-Geotail measurements, made at a separation approximately equal to the L1 distance. One may note that when Geotail is in the solar wind (outside the horizontal arrowed bar, panel 1), the agreement in all quantities is good. Figure 5 shows the result of cross-correlating the time series. The upper panel refers to the ambient solar wind intervals (excluding the sheath region of the first ICME) and the lower panel gives the result for the first ICME as a function of lag. The different parameters are shown by different colors, as explained in the upper right-hand corner of the top panel.

[25] A sharp contrast is evident between the results for the two IMF structures. In the case of the ICME 1, the cross-correlation coefficients R for all components and for the total field maximize to close to unity at about the same lag, which is slightly longer than that due to advection (R = 0.962 (B_x), 0.958 (B_y), 0.970 (B_z), and 0.974 (B) at lags of 0, 4.3, 8.6, and 4.3 min, respectively). The slopes are also similar. Under the definition of scale length introduced in section 2, we obtain similar correlation lengths of $\sim$420 R_E in the X-direction (a decrease of 0.1 in R occurs in 30 min, and we have an average bulk speed of $\sim$1500 km s^{-1}). This length scale may be considered a conservative estimate given the very high values of R. This length scale leads us to expect good correlation of these quantities between ACE and Wind as well (see below).

[26] By contrast, the swaths of ambient IMF data gives lower cross-correlations, which also differ from one component to another, and where the dependence on the lag (the "gradient") is also different. Quantities B_y and B have high correlation (R = 0.852 (B_y) and 0.894 (B) at lags of 4.3 and −2.3 min, respectively), which for B_x is fair (R = 0.640 at −8.6 min lag), while that for B_z is poor (R = 0.560 at a lag of −2.3 min). It appears from this figure that there is significant temporal and/or spatial variation in the latter two components as the IMF propagates from ACE to Geotail. One must keep in mind, however, that propagation delays for the ambient solar wind are about twice those for the ICME 1.

4.1.2. ACE-Wind

[27] We next consider the paired ACE and Wind measurements. We use the smoothing procedure on Wind data (i.e., working with 15 min averages) mentioned in the previous section. The results are shown in Figure 4 by the red traces. Also, we discuss only the clock angle of the field, θ. Using the coplanarity condition on the magnetic field at the bow shock, *Song et al.* [1992] showed that θ remains invariant across the bow shock. It is thus the parameter best suited for this comparison, since some of the Wind data are from the magnetosheath. The following points may be made from a comparison of the time profiles of θ (bottom panel). There are long intervals when there is no agreement at all. These are (1) most of the time interval up to the shock S_1, (2) most of the interval from 1200 UT (30) till soon after the arrival of shock S_2, and (3) the second half of 31 October and all of 1 November. At these times the B-panel indicates values below 10 nT so that these data represent most likely measurements inside the geomagnetic tail. Then there are two long intervals when the clock angles are similar. They occur (1) during the passage of ICME 1 and continuing after the field directional discontinuity marking our presumed end of the cloud up to 1200 UT (30) and (2) during the early part of ICME 2 including part of the sheath region. At these times the B measurements show values above 10 nT.

[28] The result of cross-correlating the clock angles for ICME 1 is shown in Figure 6. A peak cross-correlation coefficients of 0.825 is reached. While lower than those between ACE and Geotail, the cross-correlation is nevertheless good, showing that even near the L2 point the coherence of the magnetic cloud structures is retained to good approximation. A corollary of this is that a monitor at twice the distance of L1 may give good predictions of ICME-type events. We examine this point further in section 5. Note that the ICME 1 rear may have passed ACE several hours after 0200 UT (29), the time marked in Figures 1

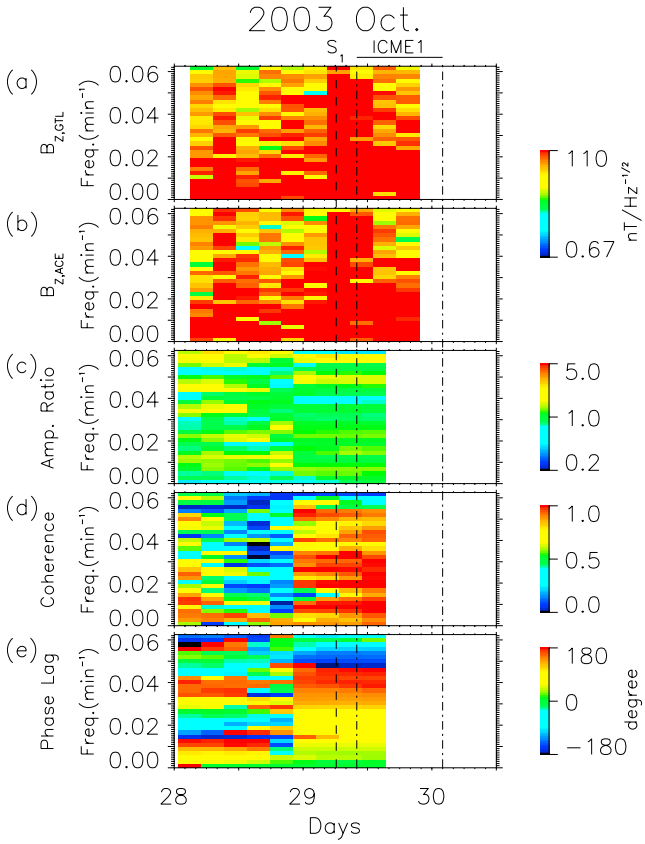

Figure 7. Spectrograms of the B_z component as measured at ACE and at Geotail for the period 28–30 October. From top to bottom are plotted the spectral density at Geotail and ACE, the amplitude ratio, the coherence, and the phase lag.

and 4. However, the clock angle panel shows continued agreement up to 1200 UT (30). We now turn to the frequency domain.

4.2. Spectral Analysis

[29] Figure 7 shows a spectral analysis on the B_z component at ACE and Geotail for the period 28–30 October, including the passage of ICME 1. At this time, Geotail was in the solar wind. Quantity B_z is arbitrarily chosen as a representative IMF component. The times of arrival of shock S_1 and the duration of the ICME 1 at ACE are marked at the top. The various panels plot the color-coded spectral density of the B_z component at Geotail (GTL) and ACE as a function of frequency and UT, the amplitude ratio, coherence, and phase difference, according to the definitions in section 2. Note that the color scales in the last two panels are linear. The most interesting feature occurs on 29 October, during the passage of ICME 1. Here, the amplitude ratio of the signal (third panel) is ~1 and the coherence is high (>0.8) up to frequencies of 0.055 min^{-1} (0.92 mHz). The phase difference varies systematically with frequency, best seen in the next figure. These features may be contrasted with the ambient solar wind interval on the previous day (28 October), where the signal coherence is high only at the lowest frequencies ($\leq$0.01 min^{-1}, i.e., 0.17 mHz) and, similarly, the phase lag varies systematically only at these low frequencies. The contrast emerging from the time series analysis may thus also be seen in the spectral analysis, with the added information that the high coherence in ICMEs is carried also by the high-frequency (short wavelength) components of the signal.

[30] We now examine the frequency dependence of the coherence and phase during the passage of the first ICME in more detail. Figure 8 shows this for the period 0000–2120 UT, 29 October, i.e., for the first ICME. ACE-Geotail coherence (top panel) and phase lag plotted are as a function of frequency. High coherence exists in the frequency interval $f \leq 0.055$ and $f \sim 0.08$ min^{-1}. The frequency gap when the coherence is low may be due to the fact that the time stationarity assumption, implicit in spectral analysis, is no longer valid.

[31] The bottom panel shows the approximately linear relationships in the frequency ranges [0, 0.04] min^{-1} from which the phase speed may be inferred (equation (4)). We

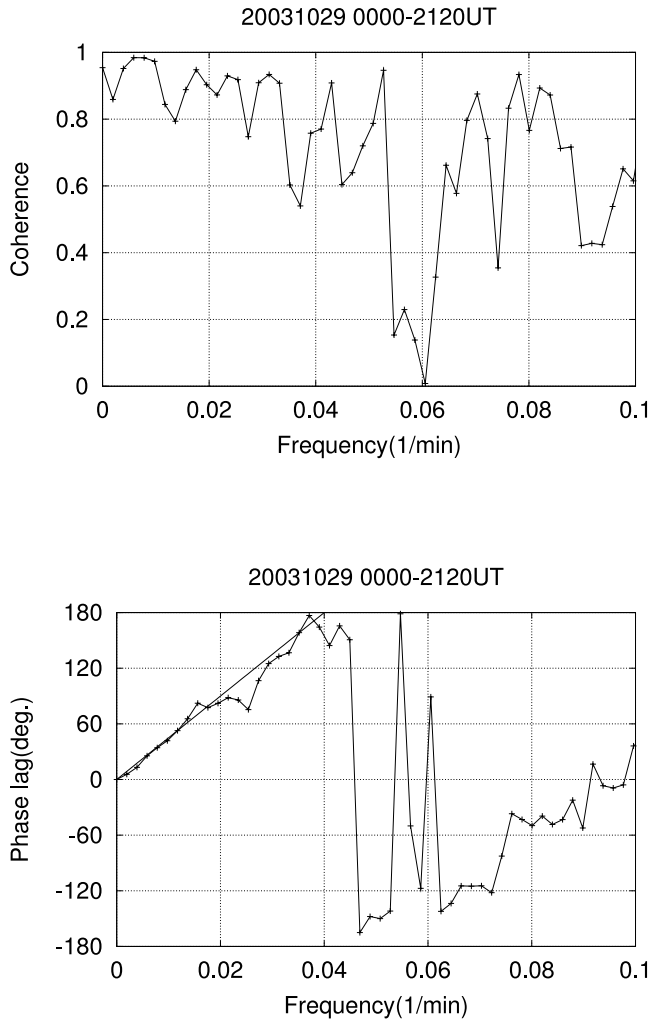

Figure 8. (top) B_z Coherence values from ACE-Geotail comparisons. (bottom) The phase lag. A straight line has been drawn through the results ACE-Geotail for $f < 0.04$ min^{-1}. The slope is proportional to the distance between the spacecraft divided by the phase speed (equation (4)).

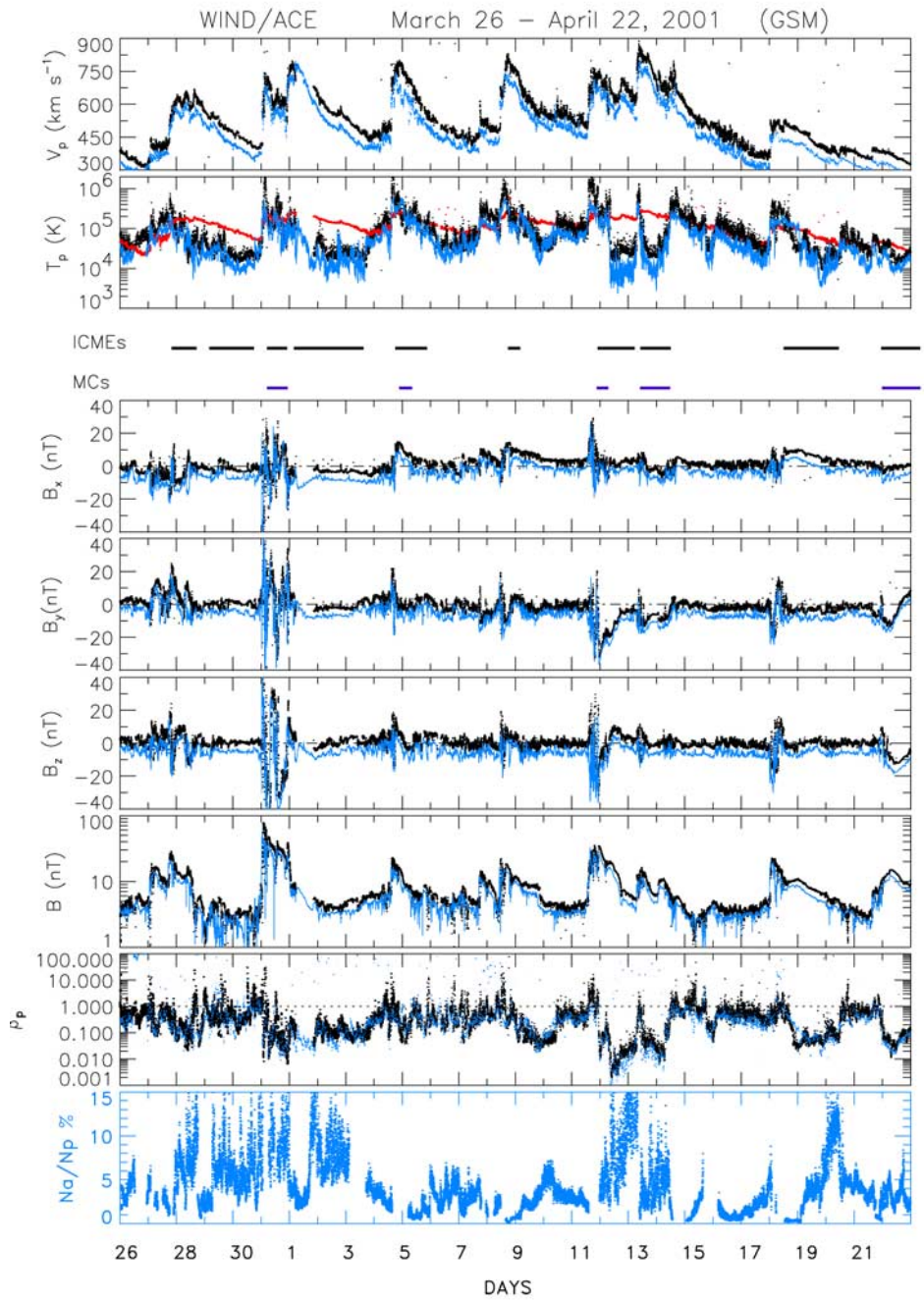

Figure 9. For the 28-day period 26 March to 22 April 2001, the figure displays time series of plasma and field parameters measured at ACE (blue) and Wind (dark trace). The ACE values have been shifted downward to permit cross-comparison. ICME and magnetic cloud (MC) intervals tabulated in the literature are shown below the second panel.

have marked in the slope for this frequency interval. The gradient of this slope equals $2\pi\Delta X/v_\phi$. With $\Delta X \approx 210\ R_E$ and a slope equal to $\pi/0.04$ rad-min, we obtain $v_\phi \approx 1700$ km s^{-1}, confirming thereby the fast propagation of this solar ejection.

[32] This was ICME 1. Geotail encountered ICME 2 when it was traveling outbound (Figure 2), crossing the bow shock at ~1130 UT (31) (Figure 4). It then follows an eastward pass where from 1500 UT (31) to ~0100 UT (1) it encounters an ~10 hour period of high-frequency variations in all magnetic field components (Figure 4). These are likely to be foreshock waves. A data gap between ~0600–0800 UT (1) is obscured by the ACE trace. The spectral analysis does not give any information because of data gap.

Halving the number of points per FFT and thereby increasing the time resolution at the expense of frequency resolution (section 1) results in no coherence at all between Geotail and ACE.

5. Broader Context: Comparison With Events of March–April 2001

[33] We now wish to inquire further into the contrasts we have found in the correlation/coherence between ICME parameters and those of the ambient IMF/solar wind for ICME 1 on a larger data set. This is necessary for three reasons: (1) The elevated speeds during the October–November 2003 events gave little time for evolution in X; (2) To investigate the correlations/coherence for ICMEs in the Y-direction. During the October 2003 events the latter aspect could not be studied because Y-separations were small. (3) To see whether high correlations is a general property of ICMEs.

[34] To this end, we examine a 28-day-long interval characterized by about 10 ICMEs. *Berdichevsky et al.* [2003] pointed out that this was a very active period on the Sun during which several CMEs were launched toward Earth. These transients were observed by both the ACE and Wind probes, each situated in the solar wind. The added advantage is that Wind was executing a distant prograde orbit carrying it far from Earth in the east-west direction. This is particularly suited for our purposes. The average separation of the IP monitors during this interval was 219 R_E (ΔX), 248 R_E (ΔY), and -18 R_E (ΔZ). We note that $\Delta Y \approx$ 250 R_E is about a factor of 3–5 longer than typical length scales of ambient IMF parameters quoted in the direction perpendicular to the bulk flow [*Crooker et al.*, 1982; *Richardson and Paularena*, 2001].

[35] Figure 9 overlays the time series of select parameters. The ACE data are at a temporal resolution of 3 s and 64 s for the magnetic field and plasma data, respectively. Wind data are at 97 s resolution for both field and plasma. The blue traces refer to the ACE measurements. The values of all parameters at the two spacecraft are so close that we had to shift the ACE data downward to enable comparison. From top to bottom are shown the bulk speed, proton temperature, the GSM components of the magnetic field, the proton beta, and the He^{++}/H^{+} density ratio. High values of this ratio are a good indicator of ejecta material in space, as are low proton temperatures and strong fields [*Gosling et al.*, 1973; *Richardson and Cane*, 1995; see also *Gosling*, 1990]. By "low" proton temperatures, we understand "low compared to usual solar wind values," the latter being shown by the red trace in panel 2 and computed after the statistical results of *Lopez* [1987].

[36] A series of about 14 shocks were observed, generally followed by plasma material of low beta ($\ll$1). Below the second panel we indicate with horizontal bars the ICME durations identified by *Cane and Richardson* [2003, Table 1] as updated by I. G. Richardson (private communication, 2005) using a wide complement of ICME signatures, including composition and charge state ratios [see *Zurbuchen and Richardson*, 2005]. The identified ejecta intervals agree well with intervals of low proton temperatures/beta, strong fields, large rotations of the magnetic field, and enhanced α-particle-proton density ratio evident in the figure. Below these, and marked "MCs," are the subset of magnetic clouds identified in this interval by *Zhang et al.* [2004]. There are 10 ICMEs, with a total duration of about one-half of the total time interval. During this interval, eight intense magnetic storms (minimum Dst* < -100 nT, where Dst* is the Dst corrected for the effects of magnetopause currents) occurred, so these are the kind of interplanetary conditions of interest to space weather.

[37] We now carry a time-series analysis of the entire 28-day period for two plasma and two magnetic field parameters. The cross-correlation coefficient plotted versus lag is shown in Figure 10 for select parameters, namely, V_p, n_p, B, and B_z. Maximum correlation of about 0.8 for both plasma and magnetic field parameters is reached at an average lag time of ~ -30 min. This lag is long presumably because the corotation time is folded into it, and it is negative because Wind is to the west of Earth, encountering the structures before a hypothetical monitor would which is located on the Sun-Earth line at equal X.

[38] Evidently, the flow field has a very large scale length. The scale lengths of the other quantities are shorter, that for B_z being the shortest. As an example of scale lengths, consider B and n_p: a decrease of R by 0.1 occurs at a lag of $\sim$1.8 hours. Using an advection speed of $\sim$600 km s^{-1}, we obtain a scale length of $\sim$600 R_E, consistent with the long scale lengths of ejecta parameters we inferred for October 2003.

[39] The absolute values of the correlation coefficients are somewhat below those of the October 2003 magnetic ICME 1 discussed earlier. This is probably due to the admixture of solar wind to the ejecta material during these 28 days, since the cross-correlations of ambient solar wind parameters are lower, as we have seen.

[40] To investigate this issue further, we now examine the time series of the the cross-correlation coefficient of B and B_z shown in Figure 11. We use 12-hour data blocks overlapped by one-half, as explained in section 2. The identified ICME and MC intervals are also indicated. One may note a generally high cross-correlation coefficient (>0.7 for $\sim$40% of the total interval), with a good association with ICME intervals. There are also clear exceptions. For example, the second (from left) ICME has a low cross-correlation coefficient in both B as well as B_z. There are also some cases where a high correlation coefficient extends to regions beyond those identified as ejecta material. The general impression is, however, that there is a pronounced tendency for sustained high correlation coefficients to be associated with the ICMEs.

[41] Finally, we consider the frequency-time spectrograms for the B_z component of the magnetic field. These are shown in Figure 12, in the same format as Figure 7. The ICME and MC intervals are noted at the top for reference. The same period (28 March to 23 April) is examined. The following points may be made. (1) The remarkable thing is that at these large separations there should be intervals of high coherence at all; (2) There is a marked tendency for enhanced spectral power together with high coherence values up to high frequencies during ejecta passages (see for example 31 March and 4 April); (3) in general, the ambient solar wind intervals show very low coherence, even at low frequencies; (4) However, once again, as in the

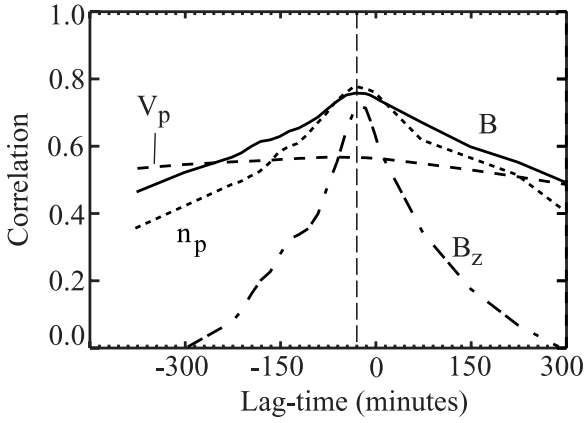

Figure 10. The cross-correlation coefficients of select magnetic field and plasma parameters for the same 28-day period as in Figure 9.

correlation analysis, there are some ICMEs where the coherence is weak (for example, 1–3 April) and others where high coherence is only maintained for part of the ejecta interval, for example, 21–23 April. We thus conclude that coherence of ejecta parameters to distances of $\sim$200 R_E in both X and Y may be considered as a property of ICMEs, though by no means shared by all these objects.

6. Summary and Conclusions

[42] We have documented correlation/coherence coefficients and length scales of magnetic field parameters during the events of 28 October to 1 November 2003. We have analyzed the data in both time and frequency domains and have considered ICME and the ambient IMF parameters separately. The latter aspect makes this, to our knowledge, the first study undertaken so far where correlation coefficients are examined in their dependence on interplanetary structures. This interval was well suited for our purposes: (1) The durations of the ambient solar wind and ICME time intervals were comparable; (2) three spacecraft were roughly equispaced over a distance in the Earth-Sun direction of $\sim$400 R_E; (3) the spread in Y was much smaller ($\leq$50 R_E).

[43] On the degree of correlation of IMF parameters, many previous studies, mentioned in the introduction, yielded correlation lengths of $\leq$200 R_E in the X-direction, the exact value depending on a number of factors which need not concern us here. When the problem is approached through spectral analysis, it is found that coherence of the two signals (in the sense of equation (2)) is mainly carried by the low-frequency components of the signals. The length scales in the X-direction inferred from spectral analysis are similar to those obtained from time series analysis.

[44] When ICME magnetic field parameters are cross-correlated, a different picture emerges. For ICME 1 a good correlation persists up to $\Delta X \sim 400$ R_E, of order the L1–L2 distance. Further, high coherence is retained over a much wider range of frequencies. Using the high coherence data, where the phase lag is also a linear function of the frequency, the phase speed of the signal can be independently obtained. For a period where this speed was exceptionally high (well in excess of 1500 km s^{-1}), we derived a value consistent with the historical values obtained by the plasma instruments on ACE and Wind.

[45] The contrast we found between ICME and ambient IMF and solar wind parameters on the 2003 period carried over to the 1 month interval in 2001. This time interval was chosen as complementary to October 2003 for three reasons: (1) there were comparable intervals of ejecta material and solar wind material; (2) spacecraft Wind was in solar wind separated by $\sim$350 R_E from ACE; (3) the spacecraft had a large Y-separation ($\approx$248 R_E). With respect to item 3, past correlation works have all emphasized the severe constraints brought about by increasing Y: values of 30–70 R_E are quoted beyond which correlations become poor, and a monitor placed at larger Y would be less likely to predict conditions at the magnetosphere well. Indeed, when we considered the ambient solar wind portions of the March–April 2001 interval, we found low coherence values, a random distribution of phase lag versus frequency, and low correlation coefficients. However, in general ICME parameters behaved differently. For most ICMEs, very good correlations were seen at the two spacecraft, implying that Y displacements of at least $\sim$248 R_E are acceptable. This would be particularly good if we placed a monitor to the west of Earth. It opens vistas of enquiry which can be followed up with joint studies of Wind, ACE, and Geotail with STEREO.

[46] A puzzling feature also emerged. While generally true, not all ICMEs had high correlation and on occasion a high correlation extended also to the neighboring solar wind. This brings in the issue of whether ICMEs are structures of low magnetic field variance.

[47] There is a general impression that the magnetic field of ICMEs and magnetic clouds is smooth. In that case, our results on high correlation/coherence would find a natural explanation and we would only have given some quantitative estimates, although these too are important. However, we believe one has to take a more differentiated view of the matter. Magnetic clouds were indeed thought to contain a smooth magnetic field [*Klein and Burlaga*, 1982; *Tranquille et al.*, 1987]. However, more recent work [e.g., *Goldstein et*

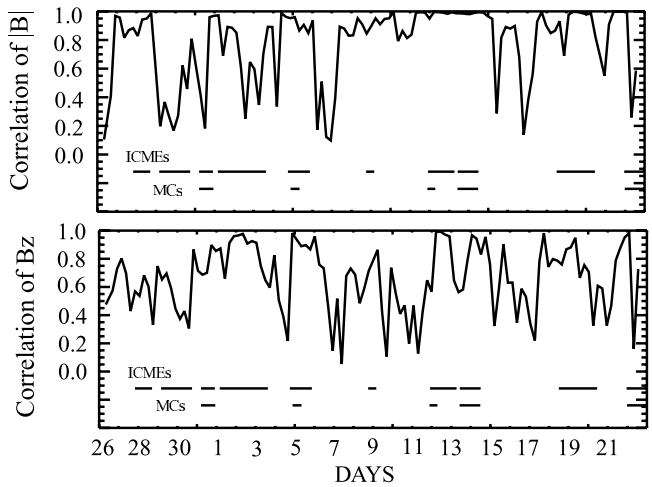

Figure 11. The cross-correlation coefficient of B and B_z for this 28-date time period.

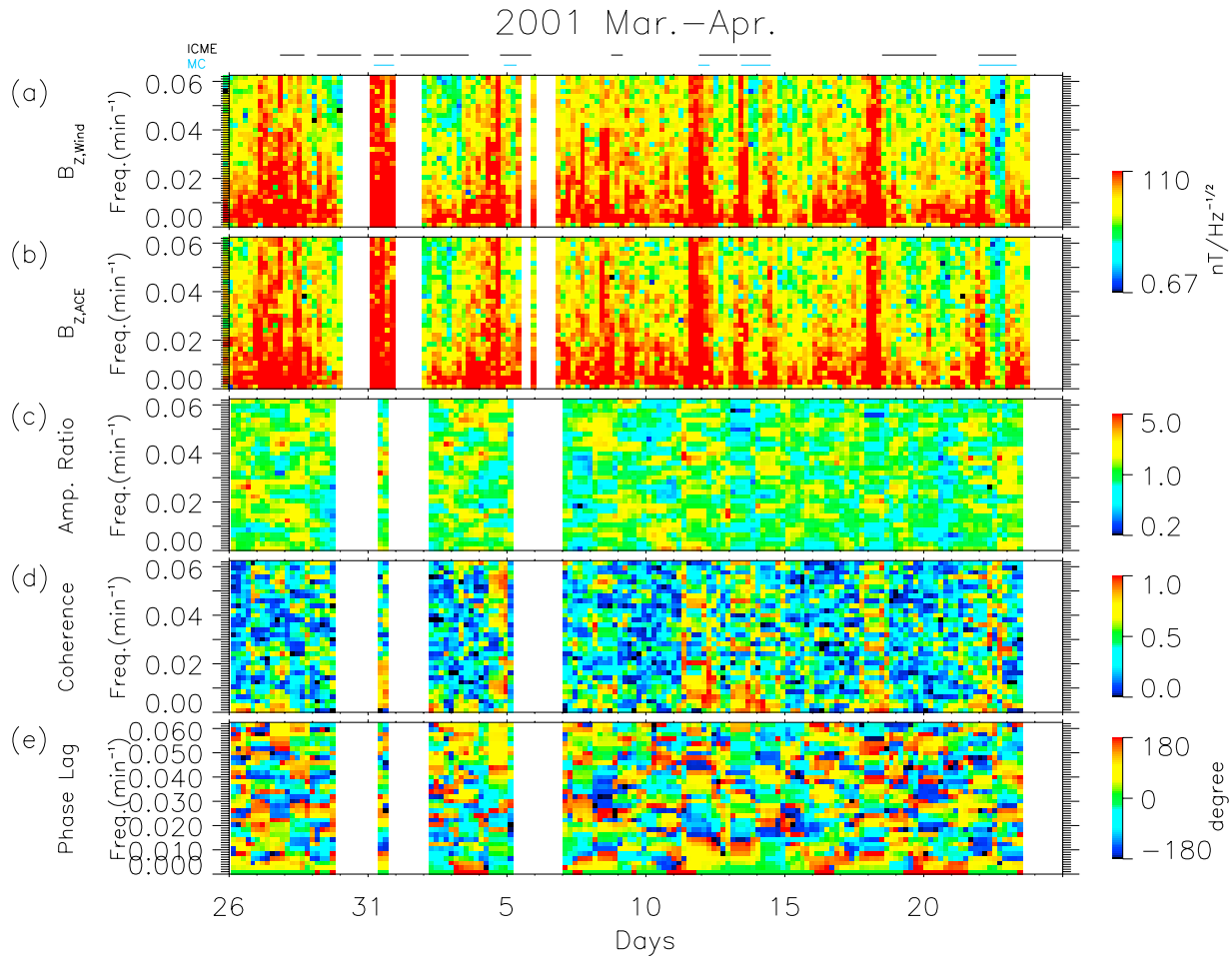

Figure 12. A spectral analysis of the same period. The format is the same as Figure 7. The magnetic component analyzed is B_z. Tabulated intervals of ICME and MC observations are shown at the top.

al., 1996; *Janoo et al.*, 1998; *Vasquez et al.*, 2001] find a surprisingly high level of magnetic field fluctuations, substructures in ejecta, and spatial inhomogeneities in some MCs. Indeed, the magnetic field of ICME 1 on 29 October 2003 (Figure 1) is not very smooth. As regards those ICMEs which are not magnetic clouds, smoothness of the magnetic field is one of several possible properties. Unfortunately, this heterogeneous bunch of objects is not distinguished by a universal set of properties (see, e.g., *Zurbuchen and Richardson*, 2005), whence stems the difficulty of identifying them. For this, and also to identify their boundaries, one uses typically the criterion of three or more signatures being present together (such as low proton temperatures, bidirectional flows of suprathermal electrons, hindrance of cosmic rays (Forbush decreases), strong magnetic fields, high He^{++}/H^{+} ratio, and so forth). Our results, based on a limited data set, indicate that the majority of ICMEs are smoother magnetically than the ambient IMF, and any inhomogeneities appear only over length scales longer than a few 100 R_E. It is a larger question well worth pursuing, but one outside the scope of this paper, to enquire why some ICMEs and magnetic clouds have low correlation/coherence.

[48] Overall, the results may be considered good news for the space weather program [see also *Coplan et al.*, 2001]. A central concern of this program is to be able to predict reliably the arrival at Earth of disruptive structures. Among all solar wind structures, ICMEs and magnetic clouds are known to lead to long and intense coupling with the magnetosphere and are thus the objects of greatest interest to this program. The ICMEs in our work were geoeffective enough to excite interest. The March–April, 2001 events gave rise to eight major geomagnetic storms (Dst* < −100 nT) of which some were "great" (Dst* < −250 nT). Some great storms followed in quick succession during mergers of ejecta (e.g., 31 March) [*Farrugia and Berdichevsky*, 2004]. Thus these would be the structures whose arrival one would wish to predict [see also *Oler*, 2004]. Here we have indications that for such structures the correlation lengths are generally longer than for ambient solar wind parameters, allowing for the placement of monitors further from Earth, with a concomitant increase in the warning time.

[49] However, we must bear in mind that the October 2003 events were fast. This means that in absolute terms the disturbances reached Earth much quicker than normal. Thus

there was not much time for evolution along X. While the results did not explicitly depend on the phase speed, it would nevertheless be desirable to examine in future work slow ICMEs/magnetic clouds when Wind is also in the magnetosheath far downstream of Earth. In that way the longer distance translates into longer lead times. Such work is under way.

[50] **Acknowledgments.** We thank Ian G. Richardson for providing us with data from work in progress and in press and for his helpful comments related to the ICMEs in March–April 2001. Geotail data are courtesy of the DARTS Web site, with special thanks to T. Nagai. This work is supported by the Wind grant NAG5-11803; NASA grant NNG05GG25G; NASA Living With a Star grants NAG5-10883, NAG5-13512, and NASW/02035; and NSF Space Weather grants ATM-0208414 and NATM-0309585. Work at Los Alamos was performed under the auspices of the U.S. Department of Energy, with financial support from the NASA ACE program.

[51] Arthur Richmond thanks Edward Smith and Steve T. Suess for their assistance in evaluating this paper.

References

Bendat, J. S., and A. G. Piersol (1971), *Random Data: Analysis and Measurement Procedures*, Wiley-Interscience, Hoboken, N. J.

Benignus, V. A. (1969), Estimation of the coherence spectrum and its confidence interval using the fast Fourier transform, *IEEE Trans. Audio Electroacoust.*, *17*, 145.

Berdichevsky, D. B., C. J. Farrugia, R. P. Lepping, I. G. Richardson, A. B. Galvin, R. Schwenn, K. W. Ogilvie, and M. L. Kaiser (2003), Solar-heliospheric-magnetospheric observations on March 23-April 26, 2001: Similarities to observations in April 1979, in *Solar Wind 10*, edited by M. Velli, R. Bruno, and F. Malara, *AIP Conf. Proc.*, *679*, 758.

Burlaga, L. F., E. Sittler, F. Mariani, and R. Schwenn (1981), Magnetic loop behind an interplanetary shock: Voyager, Helios and IMP 8 observations, *J. Geophys. Res.*, *86*, 6673.

Cane, H. V., and I. G. Richardson (2003), Interplanetary coronal mass ejections in the near-Earth solar wind during 1996–2002, *J. Geophys. Res.*, *108*(A4), 1156, doi:10.1029/2002JA009817.

Carrington, R. C. (1860), Description of a singular appearance seen in the Sun on September 1, 1859, *Mon. Not. R. Astron. Soc.*, *XX*, 13.

Collier, M. R., J. A. Slavin, R. P. Lepping, A. Szabo, and K. Ogilvie (1998), Timing accuracy for the simple planar propagation of magnetic field structures in the solar wind, *Geophys. Res. Lett.*, *25*, 2509.

Coplan, M. A., F. Ipavich, J. King, K. W. Ogilvie, D. A. Roberts, and A. J. Lazarus (2001), Correlation of solar wind parameters between SOHO and Wind, *J. Geophys. Res.*, *106*, 18,615.

Coroniti, F. V., and C. F. Kennel (1972), Changes in magnetospheric configuration during the substorm growth phase, *J. Geophys. Res.*, *77*, 3361.

Crooker, N. U., G. L. Siscoe, C. T. Russell, and E. J. Smith (1982), Factors controlling degree of correlation between ISEE 1 and ISEE 3 interplanetary magnetic field measurements, *J. Geophys. Res.*, *87*, 2224.

Eriksson, A. I. (1998), Spectral analysis, in *Analysis Methods for Multi-Spacecraft Data*, *ISSI Sci. Rep. SR-001*, pp. 5–42, ESA Publ., Noordwijk, Netherlands.

Farrugia, C. J., and D. B. Berdichevsky (2004), Evolutionary signatures in complex ejecta and their driven shocks, *Ann. Geophys.*, *22*, 3679.

Farrugia, C. J., L. F. Burlaga, and R. P. Lepping (1997), Magnetic clouds and the quiet/storm effect at Earth: A review, in *Magnetic Storms*, *Geophys. Monogr. Ser.*, vol. 98, edited by B. T. Tsurutani et al., pp. 91, AGU, Washington, D. C.

Farrugia, C. J., H. Matsui, H. Kucharek, V. K. Jordanova, R. B. Torbert, K. W. Ogilvie, D. B. Berdichevsky, C. W. Smith, and R. Skoug (2005), Survey of intense Sun-Earth connection events (1995–2003), *Adv. Space Res.*, in press.

Goldstein, M. L., D. A. Roberts, and L. F. Burlaga (1996), A comparison of two magnetic clouds, *Eos. Trans. AGU*, *77*(17), Spring Meet. Suppl., S211.

Gosling, J. T. (1990), Coronal mass ejections and flux ropes in interplanetary space, in *Physics of Flux Ropes*, *Geophys. Monogr. Ser.*, vol. 58, edited by C. T. Russell, E. R. Priest, and L. C. Lee, pp. 343–364, AGU, Washington, D. C.

Gosling, J. T., V. Pizzo, and S. J. Bame (1973), Anomously low proton temperatures in the solar wind following interplanetary shock waves: Evidence for magnetic bottles?, *J. Geophys. Res.*, *78*, 2001.

Gosling, J. T., S. J. Bame, D. J. McComas, and J. L. Phillips (1990), Coronal mass ejections and large geomagnetic storms, *Geophys. Res. Lett.*, *17*, 901.

Gosling, J. T., D. J. McComas, J. L. Phillips, and S. J. Bame (1991), Geomagnetic activity associated with Earth-passage of interplanetary shock disturbances and coronal mass ejections, *J. Geophys. Res.*, *96*, 7831.

Holmgren, G., and P. M. Kintner (1990), Experimental evidence of widespread regions of small-scale plasma irregularities in the magnetosphere, *J. Geophys. Res.*, *95*, 6015.

Janoo, L., et al. (1998), Field and flow perturbations in the October 18–19, 1995 magnetic cloud, *J. Geophys. Res.*, *103*, 17,249.

Kan, J. R., and L. C. Lee (1979), Energy coupling function and solar wind-magnetosphere dynamo, *Geophys. Res. Lett.*, *6*, 577.

Kelly, T. J., N. U. Crooker, G. L. Siscoe, C. T. Russell, and E. J. Smith (1986), On the use of a sunward libration-point-orbiting spacecraft spacecraft as an interplanetary magnetic field monitor for magnetospheric studies, *J. Geophys. Res.*, *91*, 5629.

Klein, L. W., and L. F. Burlaga (1982), Interplanetary magnetic clouds at 1 AU, *J. Geophys. Res.*, *87*, 613.

Kokubun, S., et al. (1994), The GEOTAIL Magnetic Field Experiment, *J. Geomagn. Geoelectr.*, *46*, 7.

Lepping, R. P., et al. (1995), The Wind magnetic field investigation, *Space Sci. Rev.*, *71*, 207.

Lopez, R. E. (1987), Solar cycle invariance in solar wind proton temperature relationships, *J. Geophys. Res.*, *92*, 11,187.

Malandraki, O. E., D. Lario, L. J. Lanzerotti, and E. T. Sarris (2005), October/November 2003 ICMEs: ACE/EPAM solar energetic particle observations, *J. Geophys. Res.*, *110*, A09S06, doi:10.1029/2004JA010926.

Matsui, H., C. J. Farrugia, and R. B. Torbert (2002), Wind-ACE solar wind correlations, 1999: An approach through spectral analysis, *J. Geophys. Res.*, *107*(A11), 1355, doi:10.1029/2002JA009251.

McComas, D. J., et al. (1998), Solar wind electron proton alpha monitor (SWEPAM) for the advanced composition explorer, *Space Sci. Rev.*, *86*, 563.

Ogilvie, K. W., et al. (1995), SWE, a comprehensive plasma instrument for the Wind spacecraft, *Space Sci. Rev.*, *71*, 55.

Oler, C. (2004), Prediction performance of space weather forecast centers following the extreme events of October and November 2003, *Space Weather*, *2*, S08001, doi:10.1029/2004SW000076.

Paularena, K. I., G. N. Zastenker, A. J. Lazarus, and P. A. Dalin (1998), Solar wind plasma correlations between IMP 8, INTERBALL-1, and Wind, *J. Geophys. Res.*, *103*, 14,601.

Perreault, P., and S.-I. Akasofu (1978), A study of geomagnetic storms, *Geophys. J. R. Astron. Soc.*, *54*, 547.

Press, W. H., S. A. Teukolsky, W. T. Vetterling, and B. P. Flannery (Eds.) (1992), *Numerical Recipes in C*, 2nd ed., Cambridge Univ. Press, New York.

Richardson, I. G., and H. V. Cane (1995), Regions of abnormally low proton temperature in the solar wind (1965–1991) and their association with ejecta, *J. Geophys. Res.*, *100*, 23,397.

Richardson, I. G., H. V. Cane, and E. W. Cliver (2002), Sources of geomagnetic activity during nearly three solar cycles (1972–2000), *J. Geophys. Res.*, *107*(A8), 1187, doi:10.1029/2001JA000504.

Richardson, J. D., and K. I. Paularena (2001), Plasma and magnetic field correlations in the solar wind, *J. Geophys. Res.*, *106*, 239.

Richardson, J. D., F. Dashevskiy, and K. I. Paularena (1998), Solar wind plasma correlations between L1 and Earth, *J. Geophys. Res.*, *103*, 14,619.

Russell, C. T., G. L. Siscoe, and E. J. Smith (1980), Comparison of ISEE-1 and -3 interplanetary magnetic field observations, *Geophys. Res. Lett.*, *7*, 381.

Shue, J.-H., et al. (1998), Magnetopause location under extreme solar wind conditions, *J. Geophys. Res.*, *103*, 17,691.

Skoug, R., J. T. Gosling, J. T. Steinberg, D. J. McComas, C. W. Smith, N. F. Ness, Q. Hu, and L. F. Burlaga (2004), Extremely high speed solar wind: 29–30 October 2003, *J. Geophys. Res.*, *109*, A09102, doi:10.1029/2004JA010494.

Slavin, J. A., E. J. Smith, D. G. Sibeck, D. N. Baker, R. D. Zwickl, and S.-I. Akasofu (1985), An ISEE 3 study of average and substorm conditions in the distant magnetotail, *J. Geophys. Res.*, *90*, 10,875.

Smith, C. W., J. L'heureux, N. F. Ness, M. H. Acuna, L. F. Burlaga, and J. Scheifele (1998), The ACE magnetic field experiment, *Space Sci. Rev.*, *86*, 613.

Song, P., C. T. Russell, and M. F. Thomsen (1992), Slow mode transition in the frontside magnetosheath, *J. Geophys. Res.*, *97*, 8295.

Sonnerup, B. U. O. (1974), Magnetopause reconnection rate, *J Geophys. Res.*, *79*, 1546.

Tranquille, C., T. R. Sanderson, R. G. Marsden, K.-P. Wenzel, and E. J. Smith (1987), Properties of a large-scale interplanetary loop structure as deduced from low-energy proton anisotropy and magnetic field measurements, *J. Geophys. Res.*, *92*, 6.

Tsurutani, B. T., et al. (1988), Origin of interplanetary southward magnetic fields responsible for major magnetic storms at solar maximum (1978–1979), *J. Geophys. Res.*, *93*, 8519.

Tsurutani, B. T., W. D. Gonzalez, G. S. Lakhina, and S. Alex (2003), The extreme magnetic storm of 1–2 September, 1959, *J. Geophys. Res.*, *108*(A7), 1268, doi:10.1029/2002JA009504.

Vasquez, B. J., C. J. Farrugia, S. A. Markovskii, J. V. Hollweg, I. G. Richardson, K. W. Ogilvie, R. P. Lepping, R. P. Lin, and D. Larson (2001), The nature of fluctuations on directional discontinuities inside a solar ejecta: Wind observations and theoretical interpretation, *J. Geophys. Res.*, *106*, 29,283.

Zhang, G., and L. F. Burlaga (1987), Magnetic clouds, geomagnetic disturbances and cosmic ray decreases, *J. Geophys. Res.*, *93*, 2511.

Zhang, J., M. W. Liemohn, J. U. Kozyra, B. J. Lynch, and T. H. Zurbuchen (2004), A statistical study of the geoeffectiveness of magnetic clouds during high solar activity years, *J. Geophys. Res.*, *109*, A09101, doi:10.1029/2004JA010410.

Zurbuchen, T. H., and I. G. Richardson (2005), In-situ, solar wind and magnetic field signatures of interplanetary coronal mass ejections, *Space Sci. Rev.*, in press.

D. B. Berdichevsky, R. P. Lepping, and K. W. Ogilvie, NASA Goddard Space Flight Center, Greenbelt, MD 20771, USA.

C. J. Farrugia, V. K. Jordanova, H. Kucharek, H. Matsui, C. W. Smith, and R. B. Torbert, Institute for the Study of Earth, Oceans and Space, Space Science Center, University of New Hampshire, Durham, NH 03824, USA. (charlie.farrugia@unh.edu)

J. Kasper, Center for Space Research, Massachusetts Institute of Technology, 77 Massachusetts Avenue, 37-673, Cambridge, MA 02139, USA.

T. Mukai and Y. Saito, Japan Aerospace Exploration Agency, 3-1-1 Yoshinodai, Sagamihara, Kanagawa, 229-8510, Japan.

R. Skoug, Los Alamos National Laboratory, Group ISR 1, MS D466, Los Alamos, NM 87545-0000, USA.

T. Terasawa, Department of Earth and Planetary Science, University of Tokyo, 7-3-1 Hongo Bunkyo-Ku, Tokyo, 113-0033, Japan.